Stabilization of the Hydrophilic Sphere of Iobitridol, an Iodinated Contrast Agent, as Revealed by Experimental and Computational Investigations

Dominique Meyer,[1,3] Marie-Hélène Fouchet,[1] Myriam Petta,[1] Pierre-Alain Carrupt,[2] Patrick Gaillard,[2] and Bernard Testa[2]

Received February 20, 1995; accepted June 7, 1995

Purpose. The regular distribution in space and the stability in time of the hydrophilic sphere surrounding iobitridol were investigated. This is a novel yet important concept in the design of polyiodinated contrast agents since such a sphere is meant to hide their hydrophobic core and thus prevent hydrophobic interactions with biomacromolecules and hence chemotoxicity.

Methods. The methods used were experimental (HPLC, ^{1}H- and ^{13}C-NMR spectroscopy) and computational (calculation of conformational behavior and molecular electrostatic potentials).

Results. Iobitridol exists as a mixture of stereoisomers due to hindered rotation around several bonds. High-temperature molecular dynamics established the existence between 0 and 15 kcal/mol of 238 conformers belonging to 14 classes. Most of these conformers have an inaccessible hydrophobic core, and variable temperature molecular dynamics confirmed that the hydrophilic sphere around iobitridol is stable against external disruption.

Conclusions. This study has demonstrated that iobitridol fulfills the physicochemical and structural criteria believed to render a polyiodinated contrast agent inert toward interacting with biomacromolecules.

KEY WORDS: contrast agents; molecular flexibility; variable-temperature NMR; molecular dynamics simulations; molecular electrostatic potential.

INTRODUCTION

Intermolecular interactions (recognition forces) are responsible for the exquisite selectivity of pharmacodynamic and pharmacokinetic processes. Thus, the discovery and development of therapeutic and diagnostic agents cannot be dissociated from a deep understanding of their interactions with biological sites such as proteins and membranes.

For decades, the traditional picture of the interaction between a drug and a biomacromolecule was the lock-and-key model [1,2]. However, the many advances in molecular biology and molecular pharmacology have shown how both a ligand and a macromolecule can up to a certain point adapt to each other upon binding [3]. As a result of this dynamic vision, the static lock-and-key model has now evolved to a dynamic picture of induced fit [4]. Also, the conformational flexibility of a ligand appears as an important molecular parameter whose optimization might allow some control of its interaction with binding sites [5,6]. Thus, some of us have recently demonstrated how the physicochemical and biological properties of flexible compounds can be markedly affected by their conformational state [7,8].

There is no *a priori* reason why the discovery and development of polyiodinated contrast agents, namely low osmolar contrast media (LOCMs), used in X-ray radiology should not benefit from such conceptual and methodological advances. However, and in contrast to therapeutic agents, research on contrast agents aims at minimizing their capacity to interact with biological sites and bind to them. Indeed, the interactions of LOCMs with proteins and membranes is believed to be one of the causes of their unwanted effects (chemotoxicity), the other causes being of a physicochemical nature (osmolality and viscosity) [9–12].

Because the interaction of LOCMs with biological sites is essentially of a hydrophobic nature, its intensity is proportional to the accessibility of their lipophilic zones, in particular the 1,3,5-triiodobenzene ring [13,14]. This has led to a variety of strategies to mask such lipophilic zones, mainly by introducing hydrophilic chains of an ionic (carboxylate groups) or non-ionic nature (e.g. polyhydroxylated carbamoyl groups) in positions 2, 4 and 6 of the benzene ring [15]. Originally, the effect of such vectors on hydrophilicity was assessed by measuring the global hydrophilicity of LOCMs in octanol/water or butanol/water systems or in reversed-phase HPLC. Later, more complex approaches became desirable, in particular a three-dimensional description of the topology of hydrophilic chains around the triiodobenzene ring. Indeed, there are reasons to believe that the chemotoxicity of a LOCM will be minimal if the hydrophilic contributions of the polar chains is distributed symmetrically on both sides of the triiodobenzene ring, in effect creating a *hydrophilic sphere* [14].

In addition, it has now become clear that a static view of the hydrophilic sphere is insufficient, and that the dynamic behavior of the hydrophilic substituents must also be taken into account. In other words, the aim is now to obtain a *permanent* hydrophilic sphere by designing polar chains whose conformational behavior will prevent hydrophobic forces from unmasking the triiodobenzene ring [16]. To achieve this goal, a detailed description of the dynamic behavior of LOCMs is necessary in order to understand the molecular factors that will stabilize the hydrophilic sphere.

Based on the above considerations, the novel triiodinated contrast agent iobitridol (Xenetix®) has been designed [patent EP 437144]. This compound (Figure 1) is characterized by tertiary amido groups meant to decrease the flexibility of the polar side-chains and to stabilize the hydrophilic sphere. In the present work, we investigate the dynamic behavior of iobitridol using HPLC to separate rotational isomers, variable-temperature NMR spectroscopy to determine rate constants of isomerization, and molecular dynamics to explore the conformational hyperspace.

[1] Guerbet GCA, P.O. Box 50400, F-95943 Roissy CDG Cedex, France.

[2] Institut de Chimie Thérapeutique, BEP, Université de Lausanne, CH-1015 Lausanne-Dorigny, Switzerland.

[3] To whom correspondence should be addressed.

Abbreviations: LOCM: low osmolar contrast media; MEP: molecular electrostatic potential; NMR: nuclear magnetic resonance; QMD: quenched molecular dynamics.

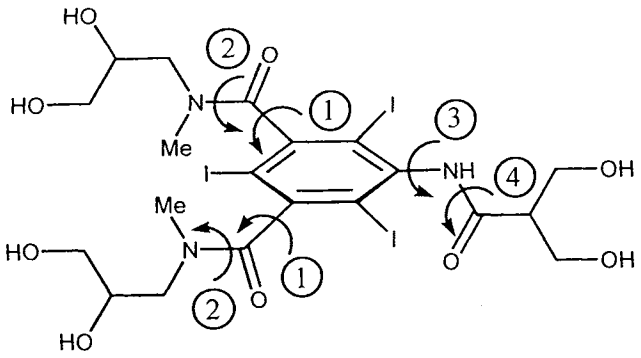

Fig. 1. Structure of iobitridol (Xenetix®) and torsion angles used to define atropisomerism.

MATERIAL AND METHODS

HPLC Experiments

Iobitridol was examined by RP-HPLC using a Lichrosphere C18 5μ phase in a 250×4mm column, and a Waters system with UV detection (240 nm). The mobile phase was made of a 0.01M NaH_2PO_4 aqueous buffer and methanol (95/5 v/v). The flow rate was 1.0 mL/min and the temperature 25 °C.

Each peak detected in analytical HPLC was isolated by semipreparative HPLC under comparable conditions. The various fractions thus obtained were immediately frozen. For the isomerization studies, each sample was heated at 100°C for 5 hours and then submitted to analytical HPLC as described above.

The identification of rotational isomers was performed by direct HPLC-MS coupling using the thermospray technique. The HPLC column (Lichrosphere C18 4μ, 150× 3.9mm) was used with a mobile phase made of a 0.1M CH_3COONH_4 aqueous buffer and methanol (93/7 v/v) (flow rate 1.0 mL/min). The MS equipment was a Nermag 10-10-L machine with quadripolar filter (range 2000 amu) and a Vestec thermospray. The operating conditions were as follows: positive mode of detection, input and output temperatures 144 and 215 °C, respectively, source temperature 245 °C, primary vacuum $8 \cdot 10^{-2}$ torr, vacuum in filter compartment $3.5 \cdot 10^{-6}$ torr.

NMR Experiments

The solutes were dissolved in D_2O or d_6-DMSO and their ^{13}C- and ^1H-NMR spectra recorded on a Bruker WM 200 spectrometer. Homonuclear spin decoupling was used for proton assignment, and the number of protons linked to each carbon was determined by pulse sequences of the type homonuclear J modulated spin echo. The assignment of carbon atoms was obtained from 2D heteronuclear experiments with a standard sequence of pulses (HETCOR) for the ^1H-^{13}C chemical shifts correlations.

To determine the free energy of activation (ΔG‡), *syn/anti* and *Z/E* isomerization equilibria were monitored by NMR using standard kinetic techniques and the well-known Eyring's equation [17]:

$$k_r = \frac{k_B T}{h} e^{\frac{-\Delta G^{\ddagger}}{RT}} \quad (1)$$

When the coalescence temperature Tc could be determined (*syn/anti* equilibria), the rate constant k_r was calculated using equation 2 where $\Delta\nu$ is the initial separation of the two coalescing peaks.

$$k_r = \frac{\pi \Delta \nu}{\sqrt{2}} \quad (2)$$

When the coalescence temperature could not be reached (*Z/E* equilibria), the rate constant k_Z or k_E was determined from the equilibrium constant K and equation 3:

$$\text{Isomer } Z \underset{k_Z}{\overset{k_E}{\rightleftharpoons}} \text{Isomer } E$$

$$k_Z = \frac{K \cdot C}{K + 1} \text{ et } k_E = \frac{C}{K + 1} \quad (3)$$

The sum of the two rate constants ($C = k_Z + k_E$) was determined graphically as the slope in equation 4 which describes the concentration variation of the two isomers as a function of time:

$$\ln\left[\frac{[Z]_t}{[Z]_t + [E]_t} - \frac{1}{K + 1}\right] = -C \cdot t + \ln\frac{K}{K + 1} \quad (4)$$

With such a method, isomerization must be monitored until equilibrium is reached [18,19].

MO Calculations of Rotation Barriers

Rotation barriers were calculated with the MOPAC 5.0 software [20] using the semi-empirical AM1 Hamiltonian. Each reaction path was explored by using steps of 10° for the rotation of each torsion angle. All other geometric parameters along the reaction paths were fully optimized using the standard criteria defined by the keyword PRECISE. The molecular mechanics correction term defined by the keyword MMOK for amide bonds was also used. Each rotation was explored independently as described in Results and Discussion. The barriers themselves were deduced graphically from the plots of heat of formation versus dihedral angle.

Molecular Dynamics and MEP

All molecular dynamics calculations were performed with the SYBYL software versions 5.5 and 6.0 (Tripos Associates, St. Louis, MO, USA) running on workstations Sun Sparc 2.0 and Silicon Graphics Personal Iris 4D/35, Power Series 4D/320 and Indigo R4000. Energy minimization was performed with the Tripos force field including the electrostatic energy term calculated from Gasteiger and Marsili atomic charges. The method of Powell was used for minimizations, convergence being reached when the gradient decrease was smaller than 0.001 kcal/mol per Å. The dynamics protocols ran automatically under commands in the SPL language of SYBYL. The molecules were compared using the option MATCH in SYBYL and taking into consideration all heavy atoms and polar hydrogens.

The method used for calculations of molecular dynamics at high temperature is similar to the QMD (quenched molecular dynamics) method [21] and consists in 4 steps using the standard SYBYL procedures except as described below:

1. Six starting geometries were selected and optimized to remove unfavorable interactions. For each geometry, a molecular dynamics simulation at 2000 K was run during 100 ps. Starting from atomic speed calculated according to a Boltzmann distribution, Newton's second equation was resolved every femtosecond. Each 0.05 ps, the conformer was stored, i.e. a total of 2000 conformers per molecule.
2. Among this number, each 10th conformer was saved in a database, i.e. 200 conformers per molecule. The geometry of each of these 200 conformers was then optimized. The optimized conformers were stored in a database and classified by increasing internal energy.
3. The pairwise comparison of the optimized conformers was performed with two criteria. Two conformers were considered as similar when a) their difference in internal energy was ≤ 3 kcal/mol, and b) the least squares difference in intramolecular distances was smaller than or equal to the means of least squares minus the standard deviation. When two conformers were considered as similar, the one with the higher energy was deleted from the database.
4. The final databases obtained from the six original geometries were pooled together and step 3 was repeated to obtain a total of 264 different conformers.

For molecular dynamics at variable temperature, the simulations were performed as follows:

1. Newton's equation was integrated every fs.
2. The coupling factor was fixed at 2 fs.
3. A first simulation at 300 K (using initial speeds calculated according to a Boltzmann distribution) was performed for 5 ps.
4. Starting from 300 K, the final temperature of 2000 K was reached by steps of 100 K during which simulations were performed for 5 ps.
5. The final simulation was performed during 500 ps. Geometries were stored each ps and their type of conformation determined automatically.

The molecular electrostatics potentials were calculated with the SYBYL software using the Coulombic approximation with the Gasteiger and Marsili partial atomic charges. The dielectric constant was $\epsilon = 1$.

Isomerism in Iobitridol

Iobitridol has two asymmetric carbon atoms but exists as an equimolar mixture of two racemates since racemic N-methylaminopropanediol is used in its synthesis. In agreement with this fact, iobitridol does not show any detectable optical activity.

In contrast, and as demonstrated below, iobitridol displays *atropisomerism*. This is due to the three iodine atoms a) inducing an orientation of the amido groups perpendicular to the plane of the ring, and b) hindering rotation of the bonds closest to the aromatic ring. Four types of bonds (bonds 1, 2, 3 and 4 in Figure 1) are involved in the atropisomerism of iobitridol.

The following nomenclature is used here to designate

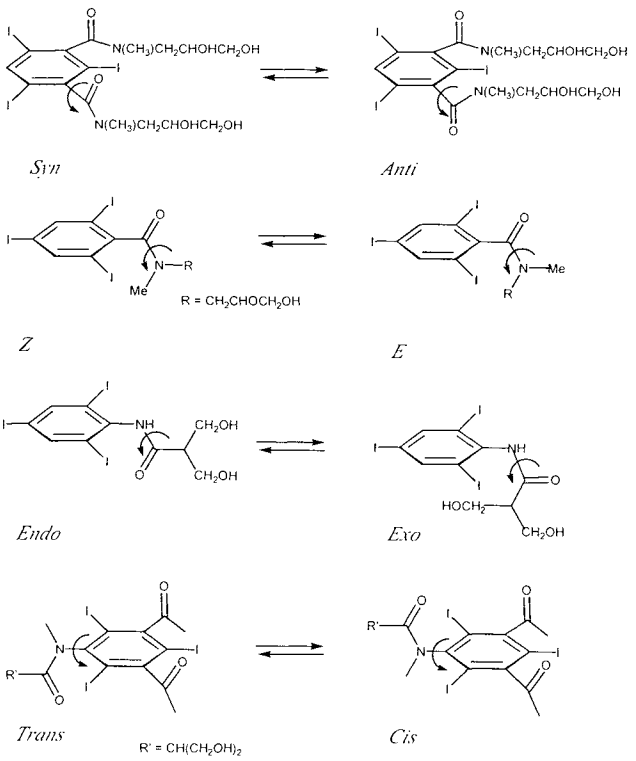

Fig. 2. Definition of the atropisomers of iobitridol.

the various conformers of iobitridol. Isomers generated by slow rotation around bond 1 are designated as *syn* and *anti* depending whether the two carbamoyl carbonyls are on the same or opposite sides of the aromatic ring (Figure 2). Isomers resulting from hindered rotation around bonds 2 and 4 are designated as *Z*/*E* and *endo*/*exo*, respectively. For a substituent of the carbamoyl type (bond 2), the *Z*-isomer has the dihydroxypropyl chain on the same side as the carbonyl oxygen (Figure 2). For a substituent of the anilido type (bond 4), the *endo*-isomer has the carbonyl oxygen pointing toward the aromatic ring.

Isomers resulting from slow rotation around bond 3 are designated here as *cis* and *trans*. This type of isomerism describes the orientation of the amido carbonyl group relative to the plane of the aromatic ring. However, *cis*/*trans*-isomerism in iobitridol exists only for *syn*-isomers since the two faces of the ring are identical in the *anti*-rotamers.

RESULTS AND DISCUSSION

Conformational Behavior of Model Compounds and Design of Iobitridol

To achieve an optimal biocompatibility of LOCMs, it is now recognized that design targets are a) a high global hydrophilicity, and b) a regular three-dimensional distribution of this hydrophilicity around the molecule. A few LOCMs have been designed according to this concept [22]. However, the *stability* of such a hydrophilic sphere has never been considered explicitly, the additional target design now being c) to obtain a hydrophilic sphere stable enough to prevent the unveiling of hydrophobic zones potentially able to elicit hydrophobic interactions with biomacromolecules.

This is the concept we have explored in designing a LOCM containing polar side-chains with hindered rotation. Amide moieties adjacent to the aromatic ring seemed a good starting point. The model compounds **1–5** (where the polar side-chains are replaced with methyl groups) were thus investigated for their barriers of rotation around bonds 1, 2, 3 and 4 (Figure 3). The calculations were performed at the semiempirical level using the AM1 method, and the results are presented in Figure 3.

In the model benzamides (compounds **1–3**), the rotation of bonds 1 was explored starting with the minimal conformations of the amide bonds 2. However, the torsion around bonds 2 was not frozen along the reaction paths. Thus as a consequence of the geometry optimizations performed at each step, the geometry around the amide function (bond 2) in compounds **2E** and **3** undergoes small modification in order to minimize steric constraints between methyl groups and iodine atoms.

For compound **2E**, the distorted geometries were the result of complex atomic changes, namely a partial rotation around bond 2 and a partial rehybridization of the nitrogen atom. These progressive deformations stopped when the relative energy became larger than ca. 20 kcal/mol; at this stage, the optimization process allowed the molecule to jump onto the rotational space of the **2Z** isomer by total rotation around bond 2. Indeed, the **2Z** stereoisomer is more stable than the **2E** isomer due to the lower steric constraints between the H atom and the iodine atoms. This behavior can explain the greater flexibility of N-monosubstituted benzamides, as seen with iopentol [19] and iohexol [23].

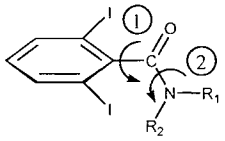

		Barrier ①	Barrier ②
1	R_1=R_2=H	12.9	14.2
2*E*	R_1=H; R_2=Me	> 20.0[a]	15.1
2*Z*	R_2=Me; R_1=H	13.7	
3	R_1=Me; R_2=Me	19.3[b]	15.0

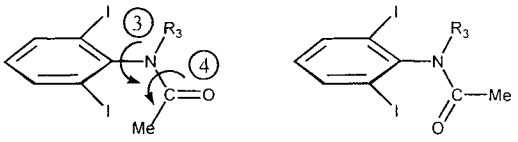

isomer *exo* isomer *endo*

		Barrier ③	Barrier ④
4*exo*	R_3=H	>14.0[a]	14.6
4*endo*	R_3=H	11.1	
5*exo*	R_3=Me	~20.0[b]	13.6
5*endo*	R_3=Me	~20.0[b]	

Fig. 3. Model compounds used for the AM1 computation of rotation barriers (indicated in kcal/mol). a) a jump to the other torsional space was observed above this energy (see Text). b) an sp^3-hybridization for the nitrogen atom was observed near the transition state (see Text).

In contrast, the amide function of compound **3** adopts a sp^3-hybridization near the transition state. An estimation of the loss in overall energy due to rehybridization should in principle be possible by calculating the barrier for compound **3** with a frozen amide function. However, the very strong interaction between methyl and iodine atoms induces other geometrical deformations (out-of-plane deviations of iodine atom, changes in bond angles around iodine atom) rendering doubtful the value of 31 kcal/mol found for this barrier. These observations imply that the barrier around bond 1 obtained for compound **3** (Figure 3) is a lower limit better reflecting an experimental situation than barriers calculated with frozen amide planar configurations.

A normal behavior was observed for the rotation around amide bond 2 starting with the minimal conformation for the bond 1. In all calculated points on the reaction path the nitrogen atom remains sp^2-hybridized. Moreover the estimated barriers are comparable with the molecular mechanics correction (14.0 kcal/mol for the N-methylacetamide) used to overcome the underestimation of this barrier by semiempirical MO calculations.

Indeed, in the model benzamides (compounds **1–3**), disubstitution of the carbamoyl nitrogen as expected induces a marked increase in the rotation barrier around bond 1, but a small increase around bond 2 (the amide bond). In contrast, monosubstitution of the nitrogen breaks the symmetry of rotation around bond 1 and enhance the flexibility due to the coupling between rotations around bond 1 and bond 2. Thus a disubstituted carbamoyl function appears to be suitable to obtain hindered rotations.

In the model acetanilides (compounds **4–5**), the rotation of bond 3 were explored starting with the minimal conformations of the amide bond 4. However, the torsion angle around bond 4 was not frozen along the reaction paths, also leading geometry variations for the amide functions. Small out-of-plane deviations of the iodine atoms were found near the transition state for compound **4endo**. In contrast, for compound **4exo**, the rotation around the bond 4 was observed allowing a jump to the most stable rotational surface of compound **4endo** when its relative energy became higher than ca. 15 kcal/mol. For the compounds **5exo** and **5endo**, the geometry of the amide bond near the transition state was largely modified, the amide loosing its conjugation and the nitrogen being sp^3-hybridized. Jumps between the two rotational surfaces were also noted for the two compounds **5exo** and **5endo**, indicating an equivalent stability of the stereoisomers with methyl substituents at both ends of the amide bond.

For acetanilides **4–5**, rotation around bond 4 starting with the minimal-energy conformation of bond 3 was as expected (sp^2 nitrogen, no deformation in geometries). Thus, substitution of the amide nitrogen induces a marked increase

in the rotation barrier around bond 3 but decreases slightly the barrier around bond 4. This decrease, together with longer synthetic routes for LOCMs of the acetanilide type, have led us to focus our interest on LOCMs with a predominance of N,N-disubstituted carbamoyl side-chains. A methyl group was selected as the second N-substituent since its hydrophobic contribution will be minimal. Indeed, the accessibility and hence hydrophobicity of such an N-methyl group is markedly reduced by the bulk of the proximal iodine atoms.

Based on these hypotheses, the novel LOCM iobitridol was designed and prepared (Figure 1, patent EP 437144). As expected, the compound proved to be highly hydrophilic ($\log P_{oct} = -2.7$). Its conformational behavior is explored here by experimental and computational techniques.

Iobitridol Exists as a Mixture of Stereoisomers

When analyzed by HPLC as described above, iobitridol elutes as 8 peaks whose UV spectra are perfectly superimposable, suggesting the existence of stereoisomers. To confirm this hypothesis, HPLC-MS experiments were undertaken. To each peak corresponded an identical mass spectrum characterized by a molecular ion [MH^+] at m/z = 836 and identical breakdown ions. In addition, the fragmentation pattern (Figure 4) is fully compatible with the molecular structure of iobitridol. These results confirm that iobitridol exists as at least 8 stereoisomers of sufficient stability to be resolvable by HPLC at room temperature.

Exploring the Conformational Hyperspace of Iobitridol and the Electrostatic Properties of its Conformers

No experimental technique exists that would allow the accessibility of the hydrophobic core of iobitridol conformers to be evaluated. We have therefore explored the conformational hyperspace of iobitridol, and calculated the three-dimensional Molecular Electrostatic Potentials (3D-MEPs) of the different conformers so obtained. Indeed, MEPs allow the characterization of regions around a molecule where polar (negative 3D-MEP) or hydrophobic (positive 3D-MEP) interactions can occur [24].

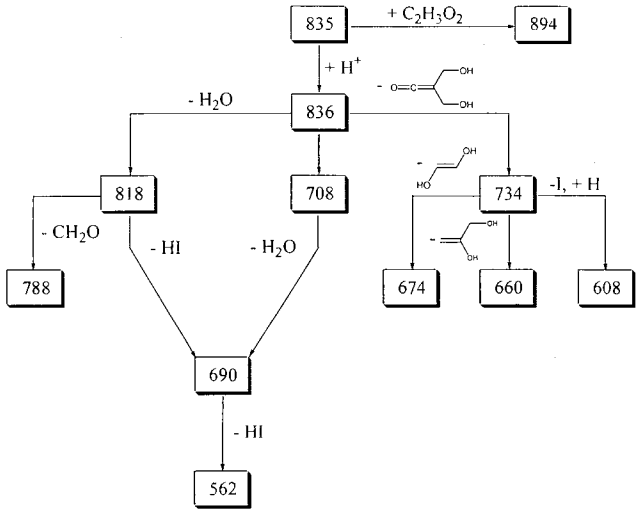

Fig. 4. Fragmentation scheme of iobitridol in mass spectrometry.

The conformers of iobitridol were generated by high-temperature molecular dynamics simulations, a computational technique well suited for complex and flexible molecules since the conformers so obtained tend to sample the property space (here the accessibility) regularly and as broadly as possible [25,26]. In the range 0–15 kcal/mol, the analysis generated 238 conformers belonging to 14 different classes. The distribution of these conformers (Table 1) shows a predominance of isomers with *endo*-geometry (90%) over those with *exo*-geometry (10%), and a predominance of *Z*-geometry (70%) over *E*-geometry (30%). In contrast, the distribution of conformers with *anti*-(53%) and *syn*-geometry (47%) is almost identical, as is the distribution of conformers with *cis*- and *trans*-geometry (56% and 44%, respectively).

The accessibility of the benzene ring in the various conformers was examined by visual inspection of their geometry and their MEP (see Figure 5 for the MEP surrounding the minimum energy conformer of iobitridol and another representative conformer). The 3D-MEPs show a regular distribution of polarity (negative MEP) around the aromatic core of the conformers resembling the minimum energy conformer represented in Figure 5b (37 % of the total number of conformers identified), as well as a markedly hydrophilic region preventing hydrophobic interactions in the conformers having an accessible aromatic core represented in Figure

Table 1. Results of the Conformational Analysis of Iobitridol by High-Temperature Molecular Dynamics

Class[a]	N[b]	E^{rel} [c]	Access[d]	3D-MEP[e]
xeest	1	8.6	+	–
x(ez)a	6	2.7-13.1	–	–
x(ez)st	1	12.5	+	–
xzza	6	3.0-11.7	–	–
xzzsc	6	7.0-10.6	+	+
xzzst	3	7.7-11.6	+	–
neea	19	2.6-13.8	–	–
neest	9	2.5-9.7	+	–
n(ez)a	52	1.5-13.8	–	–
n(ez)sc	25	3.6-14.6	+	–
n(ez)st	7	3.9-9.3	+	–
nzza	43	0-13.5	–	–
nzzsc	32	3.9-14.2	+	+
nzzst	28	1.5-11.4	+	–

[a] The various classes of conformers are defined as follows:
- *exo/endo*-atropisomerim: *x* and *n*;
- *E/Z*-atropisomerism: *e* and *z* (due to identical carbamoyl groups, the *ze* and *ez* topologies are not distinguishable and belong to the same class);
- *syn/anti*-atropisomerism: *s* and *a*;
- *cis/trans*-atropisomerism: *c* and *t*.

[b] Numbers of conformers in each class.

[c] Relative energy in kcal/mol.

[d] Facial characteristics of the 1,3,5-triiodobenzene ring:
+: at least one face of aromatic cycle is accessible;
–: both faces of the aromatic ring are hindered by hydrophilic vectors.

[e] 3D-MEP characteristics of accessible faces:
+: 3D-MEP clearly positive on the entire face, meaning that a hydrophobic interaction is possible;
–: 3D-MEP clearly negative on the entire face, implying a lack of hydrophobic interactions.

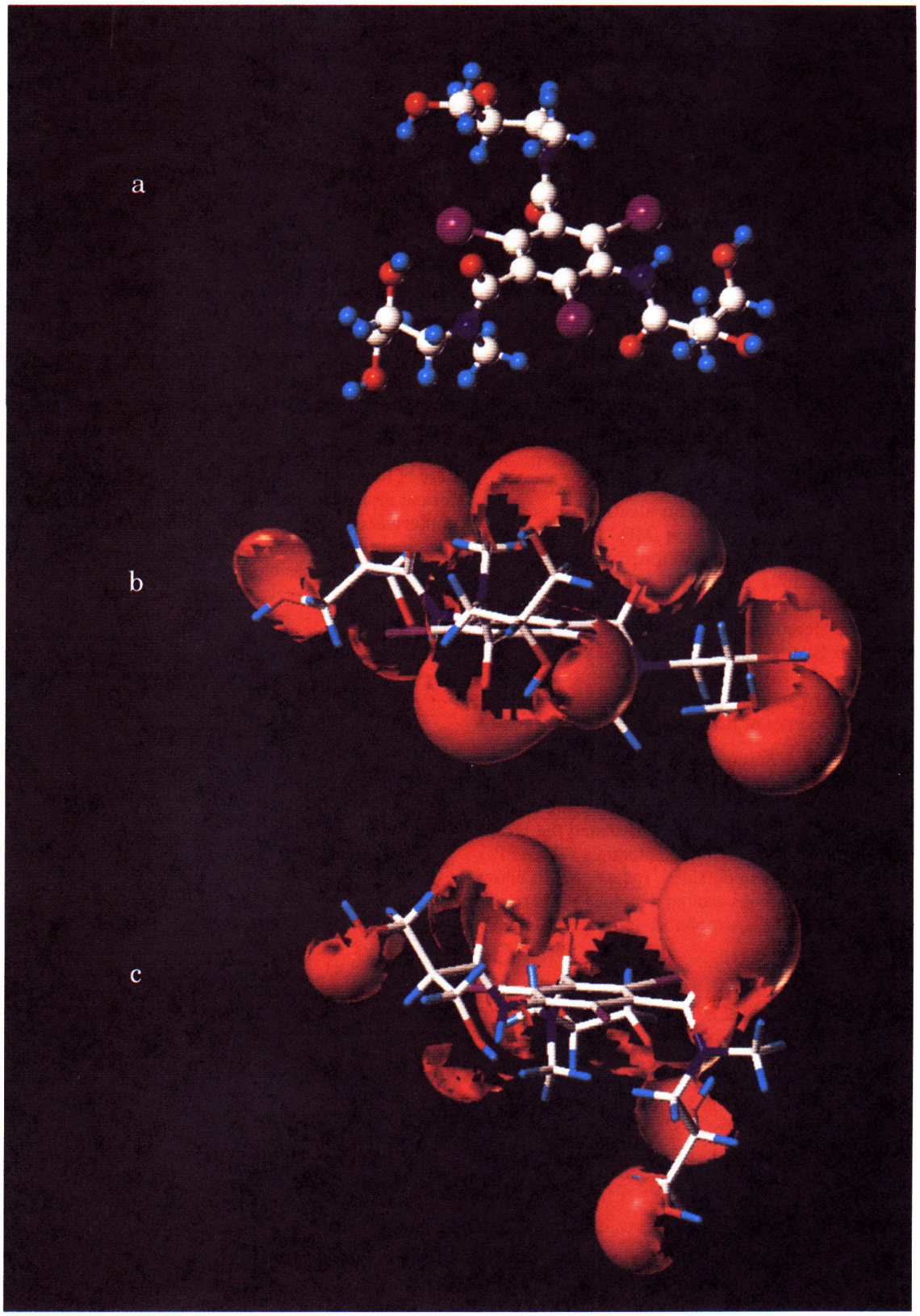

Fig. 5. (a) Three-dimensional structure of the conformer of iobitridol of lowest energy (Fig. 5a). (b) 3D-MEP distribution around the aromatic core of the lowest energy conformer; (red = negative potential, −12 kcal/mol). (c) Conformer of class ***nezsc*** characterized by a polar environment around the accessible triiodobenzene ring, a characteristic shared by the majority of conformers having a accessible face of the aromatic ring (47 % of the total number of conformers); (red = negative potential, −12 kcal/mol).

5c (47 % of the total number of conformers). Indeed, hydrophobic accessibility is found only for conformers having both carbamoyl side-chains in a *syn-Z* conformation, and an anilido side-chain in an *endo-cis* or *exo-cis* conformation. Considering the high relative energy and low frequency (16% of the total number of conformers) of the *syn-Z-*, *endo-cis-* and *exo-cis*-isomers (Table 1), they are expected to have a limited influence on the observable properties of iobitridol. A detailed NMR study of iobitridol in solution was undertaken to validate the results of the molecular dynamics simulations.

^{1}H- and ^{13}C-NMR Analysis of Iobitridol at Room Temperature

Four types of isomers can be produced by the *endo-exo-* and *cis/trans*-isomerism of the anilido side-chain around bonds 4 and 3, respectively. The complexity of the ^{1}H-NMR spectrum (Figure 6a) between 3.4 and 4.3 ppm hides the relevant information about this type of isomerism. In contrast, the simplicity of the ^{13}C-NMR spectrum (Figure 6b) of this side-chain is noteworthy, a single signal being associated with each carbon atom. This suggests either a single type of isomer or a free rotation around bond 3.

NMR data for secondary anilides show that the rotation around the aryl-NH bond is unhindered [27]. This excludes

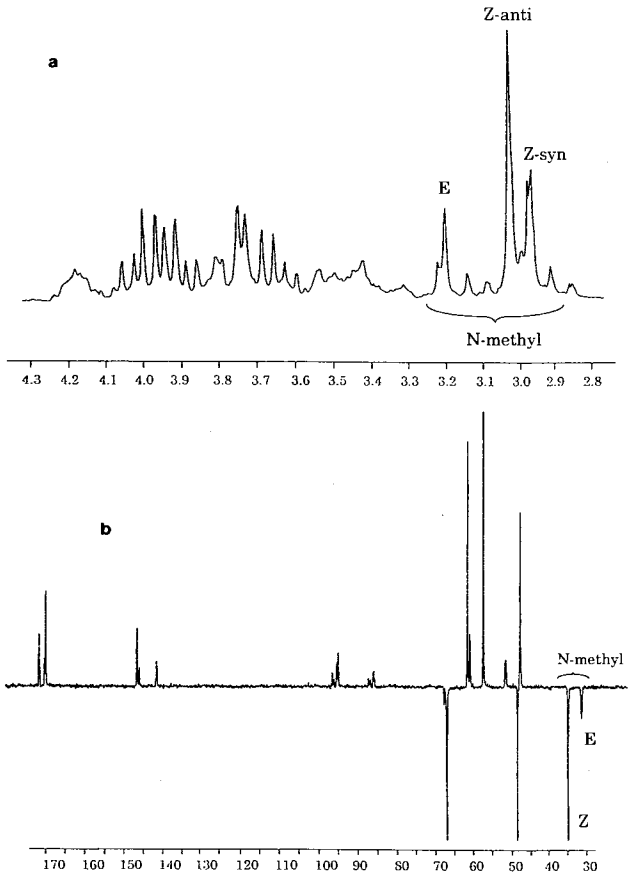

Fig. 6. (a) Partial ^{1}H-NMR spectrum of iobitridol in D_2O. The signals of the methyl groups correspond to the *E*- and *Z*-isomers and to the *syn*- and *anti*-isomers. (b) ^{13}C-NMR spectrum of iobitridol (DEPT experiment in D_2O). The signals of the methyl groups correspond to the *E*- and *Z*-isomers.

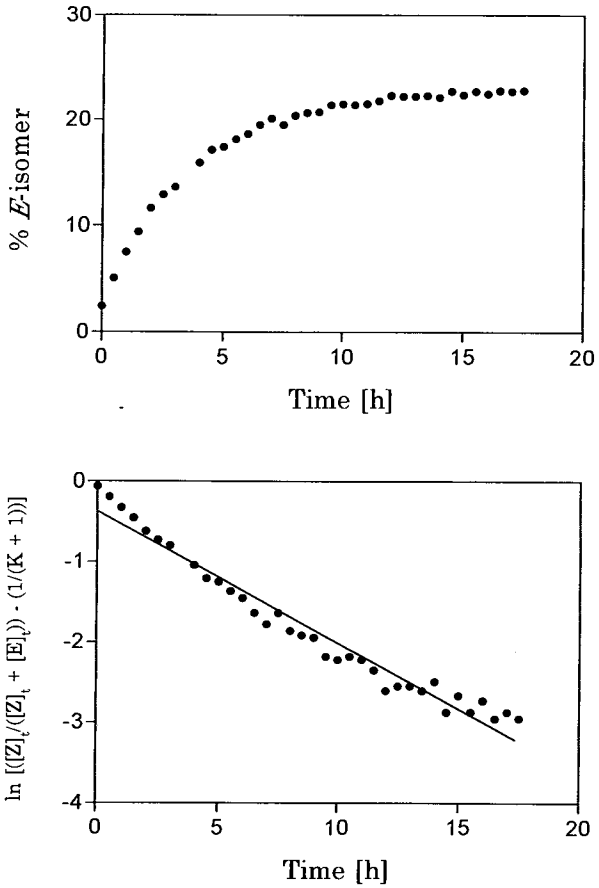

Fig. 7. *Z/E* Isomerization of iobitridol as monitored by HPLC. (a) Transformation the *Z*-isomer into the *E*-isomer. (b) Linearization according to equation (4).

the occurrence of a *cis/trans*-isomerism. In addition, bond 4 was shown to adopt the more stable *endo*-conformation [27]. The spectrum of the anilido side-chain in iobitridol is compatible with an exclusive or largely predominant *endo*-isomer, and with free rotation around the aryl-NH bond. This is in agreement with the present molecular dynamics simulations, namely large predominance of *endo*-isomers and equal proportion of *cis*- and *trans*-isomers.

For the carbamoyl side-chains, four isomers can be seen in the ^{1}H-MNR spectra, namely *syn* and *anti*, and *Z* and *E*. At room temperature, the signals of the CH and CH_2 groups appear as broad multiplets, suggesting the superposition of peaks produced by diastereomers and by rotamers. The three signals at 3.0, 3.1 and 3.2 ppm are attributed to the N-CH_3 protons by the correlation in a 2D heteronuclear NMR experiment between the two ^{13}C-NMR peaks at 31 and 35 ppm and the proton signals at 3.2 and 3.0–3.1, respectively. The existence of these three signals suggests the stability at room temperature of the isomers resulting from hindered rotation around bonds 1 and 2.

The two groups of peaks at 3.2 and 3.0–3.1 in the ^{1}H-NMR spectrum were attributed to the *E*- and *Z*-isomers, respectively. Indeed, the differences in chemical shifts must be due to different positions of the CH_3 groups relative to the aromatic ring. In the *Z*-isomer, the CH_3 group is positioned above the ring and experiences a shielding of its protons. In

the *E*-isomer, the CH_3 group is positioned away from the ring. The relative intensities of the two groups of protons confirm the distribution of isomers calculated by molecular dynamics, namely 70% *Z* and 30% *E*.

The two proton signals at 3.0 and 3.1 ppm were attributed to the *syn*- and *anti*-isomers. The 0.1 ppm difference in chemical shifts is caused by the influence of the carbonyl of one side-chain on the CH_3 group of the other side-chain. The *syn/anti*-isomerism is detectable in the NMR spectrum only for the *Z*-isomer, since the carbonyl-methyl distance is larger in the *E*-isomer and the field effect is decreased. The *syn/anti* attribution is in agreement with the almost identical proportion of *syn*- and *anti*-isomers calculated by molecular dynamics.

The distribution of isomers calculated by molecular dynamics and determined by NMR experiments implies that the desired spatial distribution of hydrophilicity around the molecule of iobitridol has been achieved. Furthermore, hindered rotation around bonds 1 and 2 suggests the stability of the hydrophilic sphere. However, an additional condition must be met, namely that supply of external energy does not perturb this hydrophilic sphere and expose the hydrophobic core. To answer this question, the dynamic behavior of iobitridol was investigated by variable-temperature NMR and HPLC experiments, and by molecular dynamics simulations over prolonged periods of time.

Experimental Studies of the Dynamic Behavior of Iobitridol

Variable-temperature NMR experiments with the pure *Z*-isomer showed that the two proton signals at 3.0 and 3.1 ppm did reach coalescence at 72°C (3.05 ppm). Using equations 1 and 2 and the difference in frequency ($\Delta\nu$ = 9.1 Hz) of the two peaks at 25°C, an activation energy $\Delta G^{\ddagger}_{345}$ = 17.3 ± 0.2 kcal/mol was calculated for the process of *syn/anti* isomerization. In contrast, no coalescence was observed for the proton signals at 3.05 and 3.2 ppm even at 140°C, indicating that the *Z/E* interconversion is highly hindered in iobitridol. This isomerization was monitored by HPLC by heating samples at 80°C for 22 h (Figure 7a). The equilibrium (K = 0.3) was reached in 12 h. A plot of equation 4 (Fig. 7b) yields the slope C (i.e. the sum of the two rate constants $k_Z + k_E$). From equations 3 and 1, one can then calculate the rate constant $k_E = 1.42 \cdot 10^{-5}$ mol^{-1} s^{-1} and the free energy of activation of the reaction, $\Delta G^{\ddagger}_{353}$ = 27.6 ± 0.2 kcal/mol at 80°C.

These results demonstrate how the tertiary carbamoyl groups in iobitridol strongly decrease its conformational freedom. Indeed, their *Z/E* isomerization is much more difficult than in secondary carbamoyl groups ($\Delta G^{\ddagger}_{383}$ = 20.0 kcal/mol [27]) and even their *syn/anti* isomerization is slightly more difficult than around secondary carbamoyl groups ($\Delta G^{\ddagger}_{333}$ = 17.4 kcal/mol [27]).

Molecular Dynamics Simulations

The relatively free rotation around bond 3 allows easy *cis/trans* isomerization. Since conformers of the classes *xzzsc* and *nzzsc* (see Table 1 for definition) have a more accessible hydrophobic core, it was deemed important to examine the molecule in its globality to see whether the population of these conformers could increase with time due to restricted rotations around the other bonds.

In the absence of a suitable experimental technique, and in view of the good agreement noted above between high-temperature dynamics simulations and equilibrium NMR, we performed variable-temperature molecular dynamics simulations to answer this question.

From each of the 14 classes of conformers identified and listed in Table 1, the minimum-energy conformer was taken and the evolution of its geometry monitored during 500 ps at temperatures of 500, 600, 700, 800, 900, 1000 and 1100 K as described under Materials and Methods.

For all starting geometries, a temperature above 500 K proved necessary to see substantial conformational changes. Interestingly, a fast *exo/endo* isomerization leading to a predominance of *endo*-conformers was seen, the *exo*-conformers being rapidly transformed into *endo*-conformers. Increasing the temperature allowed *endo*-to-*exo* isomerization to be observed, but only to a very limited extent, whereas slow *syn/anti* and *Z/E* equilibria occurred at high temperatures (>900 K). However, no evolution toward conformers of the types *nzzsc* or *xzzsc* were observed whatever the starting geometry and the temperature.

These results confirm that the carbamoyl groups in iobitridol experience highly restricted rotations that stabilize its hydrophilic sphere against external disruption.

CONCLUSION

The study reported here demonstrates that iobitridol exists as a mixture of conformers stabilized by hindered rotation around critical bonds, in particular tertiary carbamoyl moieties whose methyl groups do much to achieve this rigidification. The conformers characterized are predominantly *endo*- and *Z*-isomers, and most of them display a hydrophilic sphere that surrounds and essentially masks the hydrophobic core. As a result of the rigidity of these isomers, the hydrophilic sphere will resist perturbation by an external hydrophobic agent. The very low partition coefficient of iobitridol affords a further proof that the compound cannot unmask its hydrophobic core in hydrophobic solvents.

Thus, the potential of iobitridol to interact with hydrophobic sites in biomacromolecules should be very low. Such a behavior is considered desirable in the new safety paradigm of polyiodinated contrast agents.

ACKNOWLEDGMENTS

P.A.C. and B.T. are grateful to the Swiss National Science Foundation for support.

REFERENCES

1. R. R. Neubig and W. J. Thomsen, How does a key fit a flexible lock? Structure and dynamics in receptor function. *BioEssays* 11:136–141 (1989).
2. P. Nagy and G. Naray-Szabo, Electrostatic lock-and-key model for the analysis of inhibitor recognition by dihydrofolate reductase. *Can. J. Chem.* 63:1694–1698 (1985).
3. N. C. Khanna, M. Tokuda, and D. M. Waisman, Conformational changes induced by binding of divalent cations to calregulin. *J. Biol. Chem.* 261:8883–8887 (1986).

4. W. L. Jorgensen, Rusting of the lock and key model for protein-ligand binding. *Science* **254**:954–955 (1991).
5. P. M. Dean, P. L. Chau, and M. T. Barakat, Development of quantitative methods for studying electrostatic complementarity in molecular recognition and drug design. *J. Mol. Struct. (THEOCHEM)* **256**:75–89 (1992).
6. M. D. Walkinshaw, Protein targets for structure-based drug design. *Medicinal Res. Rev.* **12**:317–372 (1992).
7. P. A. Carrupt, B. Testa, A. Bechalany, N. El Tayar, P. Descas, and D. Perrissoud, Morphine 6-glucuronide and morphine 3-glucuronide as molecular chameleons with unexpected lipophilicity. *J. Med. Chem.* **34**:1272–1275 (1991).
8. P. Gaillard, P. A. Carrupt, and B. Testa, The conformational-dependent lipophilicity of morphine glucuronides as calculated from their molecular lipophilicity potential. *Bioorg. Med. Chem. Lett.* **4**:737–742 (1994).
9. R. Eloy, C. Corot, and J. Belleville, Contrast media for angiography: physicochemical properties, pharmacokinetics and biocompatibility. *Clin. Mat.* 7:89–197 (1991).
10. A. M. Melkumyants and S. A. Balshov, Effect of blood viscosity on arterial flow induced dilator response. *Cardiovas. Res.* **24**:165–168 (1990).
11. J. Ueda, A. Nygren, P. Hansell, and U. Erikson, Influence of contrast media on single nephron glomerular filtration rate in rat kidney. *Acta Radiologica* **33**:596–599 (1992).
12. M. Sovak, R. Ranganathan, J. H. Ling, and E. C. Lasser, Concepts in design of improved intravascular contrast agents. *Ann. Radiol.* **21**:283–289 (1978).
13. T. Prangé, F. Gaudey, J. Ohanessian, D. Avenel, A. Neuman, C. Corot, and D. Meyer, Angiography contrast agents interact with serine proteinases. The molecular structure of the model system elastase/iohexol. *FEBS. Lett.* **357**:247–250 (1995).
14. B. Bonnemain, D. Meyer, M. Schaefer, M. Dugast-Zrihen, S. Legreneur, and D. Doucet, New iodinated, low-osmolar contrast media. A revised concept of hydrophilicity. *Invest. Radiol.* **25**:S104–S106 (1990).
15. G. B. Hoey and K. R. S. Smith. Chemistry of X-ray contrast media. In M. Sovak (ed.), *In: Radiocontrast Agents*. Springer-Verlag, Berlin, 1984, pp. 23–125.
16. W. Blokzijl and J. B. F. N. Engberts, Hydrophobic effects. Opinions and facts. *Angew. Chem. Int. Ed. Engl.* **32**:1545–1579 (1993).
17. H. Kessler, Detection of hindered rotation and inversion by NMR spectroscopy. *Angew. Chem. Int. Ed. Engl.* **9**:219–235 (1970).
18. H. A. Staab and D. Lauer, Stabile rotationisomere carbonäureamide. *Chem. Ber.* **101**:864–878 (1968).
19. A. Berg and R. Fagervoll, Synthesis, isomerism and characterization of iopentol. *Acta Radiologica* **Supp. 370**:13–21 (1987).
20. J. J. P. Stewart, MOPAC: a semiempirical molecular orbital program. *J. Comput.-Aided Mol. Des.* **4**:1–103 (1990).
21. S. D. O'Connor, P. E. Smith, F. Al-Obeidi, and B. M. Pettitt, Quenched molecular dynamics simulations of tuftsin and proposed cyclic analogues. *J. Med. Chem.* **35**:2870–2881 (1992).
22. M. Sovak, The need of improved contrast media. Ioxilan: updating design theory. *Investigative Radiology* **23**:S79–S83 (1988).
23. S. J. Foster and M. Sovak, Isomerism in iohexol and ioxilan. Analysis and implications. *Investigative Radiology* **23**:S106–S109 (1988).
24. I. Alkorta and H. O. Villar, Molecular electrostatic potential of D_1 and D_2 dopamine agonists. *J. Med. Chem.* **37**:210–213 (1994).
25. G. Klebe and T. Mietzner, A fast and efficient method to generate biologically relevant conformations. *J Comput.-Aided Mol. Des.* 8:583–606 (1994).
26. C. Altomare, S. Cellamare, A. Carotti, G. Casini, M. Ferappi, E. Gavuzzo, F. Mazza, P. A. Carrupt, P. Gaillard, and B. Testa, X-ray crystal structure, partitioning behavior and molecular modeling study of piracetam-type nootropics: insights into the pharmacophore. *J. Med. Chem.* **38**:170–179 (1994).
27. S. Bradamante and G. Vittadini, Non-ionic X-Ray contrast agents: detection of ambient temperature isomers of congested hexasubstituted benzenes with multipositional hindered rotations. *Magn. Reson. Chem.* **25**:283–292 (1987).